A VISUALIZATION TOOL FOR GLOBAL ASSESSMENT OF BRONCHIECTASIS AND LOCAL EVALUATION OF THE AIRWAYS

B. L. Odry*,**, A. P. Kiraly*, C. L. Novak*, J–F. Lerallut**, D. P. Naidich***

* Siemens Corporate Research / Intelligent Vision and Reasoning Department, Princeton, NJ, USA
** Université de Technologie de Compiègne / Département Génie Biologique, Compiègne, France
*** New York University School of Medicine / Radiology Department / New York, NY, USA

benjamin.odry@siemens.com

Abstract: Bronchiectasis is a permanent dilation of the airways, usually due to chronic infection or cystic fibrosis, and Computed Tomography (CT) is the primary means by which bronchiectasis is evaluated. The introduction of multislice CT machines, allowing acquisition of near-isotropic volume data, allows accurate evaluation of airway diameters even when the airways are not perpendicular to the axial plane. However the large number of slices per patient in such datasets makes it difficult for physicians to systematically evaluate the extent of disease. We have developed a tool for airway evaluation that allows rapid determination of bronchiectasis location and extent.

Introduction

The introduction of multislice CT machines, allowing acquisition of near-isotropic volume data, should allow accurate evaluation of airway diameters even when the airways are not perpendicular to the axial plane. However it is extremely difficult for physicians to determine the true cross-section of an airway without computer assistance. Furthermore, the large number of slices per patient in multislice datasets makes it difficult for physicians to systematically evaluate the extent of disease.

Bronchiectasis is a disorder that damages and weakens the bronchial walls causing the airways to become permanently enlarged. Bronchiectasis may be congenital, or may be the result of chronic infection of the airway. Cystic fibrosis causes about 50% of all bronchiectasis in the US. In healthy lungs, the airway diameters become smaller with succeeding generations, whereas in bronchiectasis the airway lumens will fail to taper. Furthermore, the bronchial tree parallels the pulmonary artery tree, and in healthy lungs an airway will have approximately the same diameter as the accompanying artery. A broncho-arterial ratio greater than one is an indicator of the presence of bronchiectasis [1].

A computerized method for visualizing the presence and extent of bronchiectasis must begin with an automatic extraction of the bronchial tree. Various methods have been proposed in the literature for airway segmentation [2-6]. One method is based on adaptive region growing from a seed point [2]. Morphology-based methods [3, 4] have also been proposed. These approaches can yield detailed segmentations but often require around one hour of processing. In addition, the operators are applied to the entire lung region at multiple scales to attempt to segment airways in all size ranges. A combinational approach based on an initial adaptive region growing followed by smaller scale morphology was proposed in [2]. Although still applied to the entire image, only smaller airways are considered. A tracking-based approach was presented in [5]. In this segmentation, the entire airway tree is tracked from the trachea to terminal branches. Again, the method must adapt to the several different scales present in these generations. Finally, a level-set based approach on analyzing the shape of the front was proposed in [6].

Furthermore, a few systems [7, 8] provide automated assessment of airway parameters such as airway lumen diameter, airway wall diameter and/or airway broncho-arterial ratio but, besides plots, lack any associated visualization to localize abnormalities.

Based on an adaptive region growing approach, we have developed an interactive tool for airway evaluation that allows:

1) rapid determination of the location and extent of airway abnormalities
2) objective and repeatable measurements of airway dimensions
3) evaluation of changes in patient airways over time

Materials and Methods

Material

We use CT data from a 16-slice detector (Siemens Medical Solutions, Forchheim, Germany) which provides essentially isotropic resolution as the slice spacing (0.5-0.7mm) is in the same range as the in-plane resolution. The data is acquired with standard dose (200 mAs) and reconstructed using a sharp kernel. The evaluation system runs on a Pentium III Workstation, 1.7 GHz, with 2 GB of memory.

Method for airway tree visualization

The system begins by automatically segmenting the airway tree with three dimensional (3D) region growing, using adaptive thresholding, filtering, and leak detection. The region growing starts from a seed point

ISSN: 1727-1983

in the trachea that is automatically determined by labeling the air-like regions around the center of the first few slices and looking for stability in region size across slices. Size stability is determined using a tolerance ξ on the size variation.

$$S_{i+1} - S_i < \xi \quad \text{with } S_i \text{ and } S_{i+1} \text{ areas of slice } i \text{ and } i+1 \tag{1}$$

The inner bronchial diameter is computed at each point in the tree with the help of a Euclidean distance map transformation of the segmentation. The extracted airway tree is colored based upon the computed cross-sectional diameters and rendered within a 3D interactive display as shown in Figure 1. The user can zoom, pan and rotate this display.

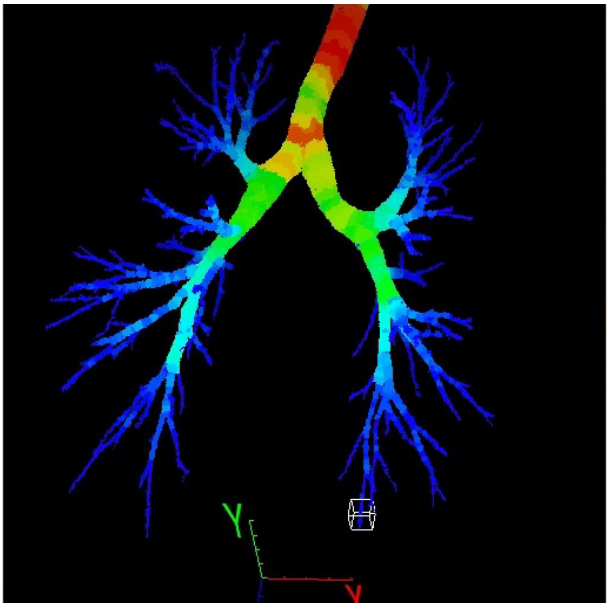

Figure 1: Airway tree for a patient with mild bronchiectasis: color-coding represents the different diameters, ranging from red (>10mm diameter) to violet (0.1mm). The white box indicates an airway selected for local evaluation.

By using a slide bar, the user can adjust the maximum diameter colored on the visualization (Figure 2). This allows a better use of the color range for the airways beyond the trachea and main bronchi, and therefore makes it easier to find dilated or non-tapering airways throughout the bronchial tree.

Method for local airway evaluation

Given a user-indicated point within the visualized airway tree, our system automatically determines the long axis of the corresponding airway by computing the eigenvectors of the Hessian matrix of the original data around the selected point. The Hessian matrix $H(f)$ is comprised of second-order partial derivatives of a real-valued volume $f : \Re^3 \rightarrow \Re$ of the form:

Figure 2: Same airway tree as displayed in Figure 1 with a lower diameter color limit. The excluded diameter points are colored gray and the small airways show better color resolution, improving bronchiectasis assessment.

$$H(f) = \begin{bmatrix} \frac{\partial^2 f}{\partial x_1^2} & \cdots & \frac{\partial^2 f}{\partial x_1 \partial x_2} & \cdots & \frac{\partial^2 f}{\partial x_1 \partial x_3} \\ \frac{\partial^2 f}{\partial x_2 \partial x_1} & \cdots & \frac{\partial^2 f}{\partial x_2^2} & \cdots & \frac{\partial^2 f}{\partial x_2 \partial x_3} \\ \frac{\partial^2 f}{\partial x_3 \partial x_1} & \cdots & \frac{\partial^2 f}{\partial x_3 \partial dx_2} & \cdots & \frac{\partial^2 f}{\partial x_3^2} \end{bmatrix} \tag{2}$$

We can determine the plane of the airway's true cross-section with the eigenvectors.

Using the cross-sectional plane, the airway's inner and outer diameters are computed via the data obtained at the cross-section of the selected point [9]. Data is collected along multiple rays around the center of the airway on the segmented binary tree as well as the original grayscale image. An operation based on the Full Width Half Maximum (FWHM) method then computes the inner and outer diameters of each ray.

The inner diameter measurements are first approximated by the binary segmented tree. The algorithm then finds the first local maximum past this approximation within the grayscale data. Next, the two local minima about the local maximum are found. The inner and outer wall locations are determined by finding the location of the gray levels half way in between those of the local maximum and minima.

ISSN: 1727-1983

It is also possible for the user to select an airway outside of the segmentation. In this situation, an estimate of the inner airway segmentation is used for the binary segmentation. This estimate is based on a local thresholding of the original data within the click point.

We further localize the adjacent artery using a score based on its cross sectional shape, position, and long axis similarity with that of the airway, and determine its cross-sectional diameter. On the cross-sectional plane, the system labels the regions of high intensity and computes a score based on the region's circularity, similarity with the airway and proximity to the airway. This process is detailed in the following paragraphs.

The similarity parameter describes the similarity of direction and is computed by using a normalized dot product between both long axes, scaled to lie between 0 and 1. Ideally the airway and its adjacent artery are parallel; we allow a 15% difference when selecting the matching vessel.

$$similarity = \frac{1}{\sqrt{\sum_{j=0} x_j^{\,2}} \cdot \sqrt{\sum_{j=0} y_j^{\,2}}} \sum_{i=0}^{2} \left| x_i . y_i \right| \qquad (3)$$

with x_i and y_i being the long axis of the vessel and airway respectively

Since the cross section of a vessel should be roughly circular, we compute a circularity operator, which is a ratio between the area of the structure and the corresponding disc defined by the maximum diameter of the structure.

$$circularity = \frac{N}{\pi \cdot R\max^2} \qquad (4)$$

with N the number of pixels of the structure and *Rmax*

Finally, the adjacent vessel is generally close to the airway. The last indicator is a distance ratio between the airway inner diameter and the distance between the airway and artery centers.

$$proximity = \frac{D_{airway}}{Dist} \qquad (5)$$

with D_{airway} the airway outer diameter, *Dist* the distance between the center points of the airway and artery.

Once the corresponding artery to an airway has been determined, the artery diameter can be compared with the airway diameter to indicate airway dilation, as shown in Figure 3.

Method for monitoring airway changes over time

Our system also offers a follow-up feature: Two datasets from the patient, acquired at different time points, are simultaneously loaded for analysis (Figure 4). This allows the user to rapidly evaluate whether a patient's disease is progressing or responding to treatment.

The user may select an airway in either the first or second dataset and the computer will automatically localize the same airway in the other dataset. This is accomplished by first performing an approximate global registration of the lungs in each dataset [12], based on linear equation fitting to the cross-sectional area of the lungs in each orthogonal direction (axial, sagittal, coronal). Next, for each user-selected point in an airway, the system performs a local search to determine the corresponding airway structure that is the closest match

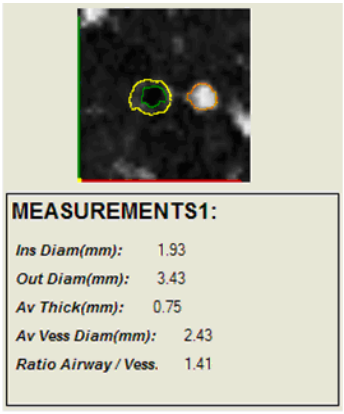

Figure 3: Local evaluation of the airway, shown in the plane perpendicular to the airway. The inner (green) and outer (yellow) diameters of the airway are shown along with the extracted measurements. The adjacent artery diameter is outlined in orange, and the airway/artery ratio is indicated. A ratio greater than one may indicate that the airway is abnormally dilated.

Given the airway in each dataset, the system extracts the airway diameter and wall thickness for both time periods, using the same techniques previously described. An example is shown in Figure 5. The matching and measurement process take less than one second for each location, allowing the user to rapidly evaluate changes in the airways.

Results

We analyzed 10 high-resolution datasets from a radiology practice. Two out of ten datasets were acquired with the application of contrast agent. Some patients were primarily scanned for airway diseases in general (cystic fibrosis, emphysema, hemoptysis), while others were scanned for screening purposes.

For different reasons, such as airway wall thickening, mucoid impaction, and noise, the automatic segmentation is not always able to reach beyond the 5th generation airways. This is especially true for those cases *without* bronchiectasis, where the airways rapidly become smaller with succeeding generations. Indeed, the number of airway generations included in an

ISSN: 1727-1983

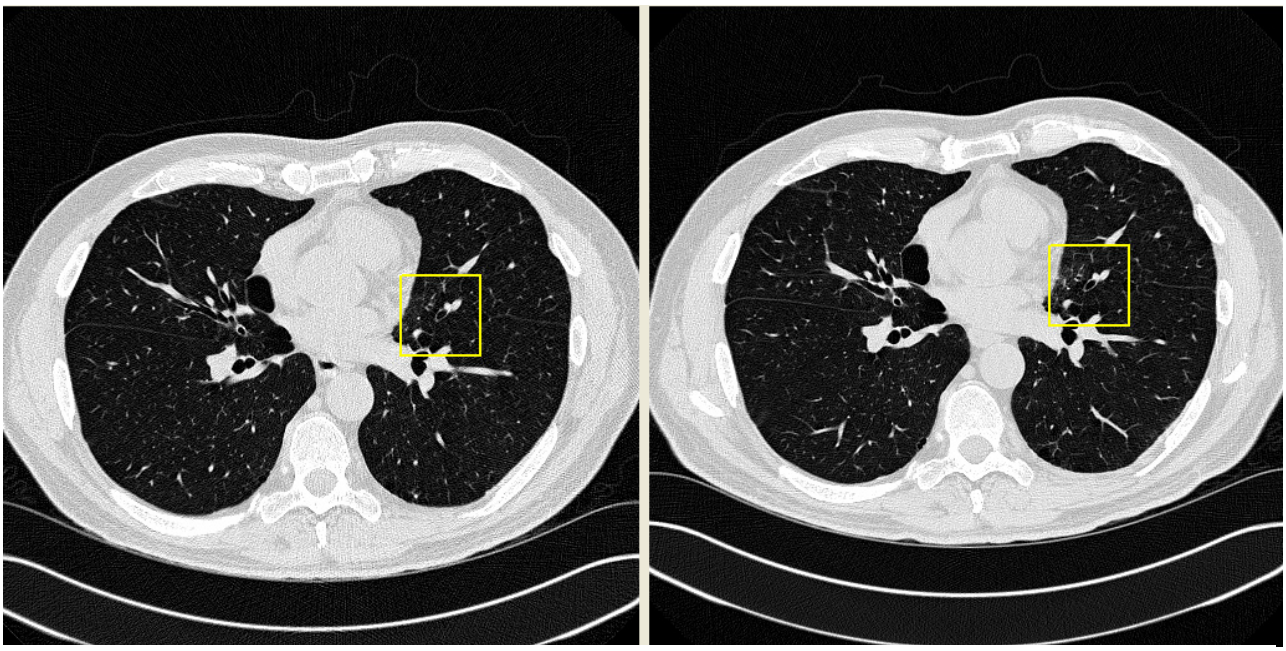

Figure 4: CT datasets of the same patient, acquired 116 days apart. The user clicked an airway in the earlier dataset on the left, as indicated by the yellow box. The computer automatically computed the matching airway, indicated by the yellow box on the right.

automatic segmentation may ultimately prove a useful indicator for the presence of bronchiectasis. Three datasets did not have satisfying segmentation to test the visualization tool.

However, even in cases with limited generations of automatically extracted airways, the system is still capable of giving local measurements of the airway outside of the segmentation (see Figure 6a and b) and verify, depending upon the disease, whether there is airway wall thickening or elevated broncho-arterial ratio.

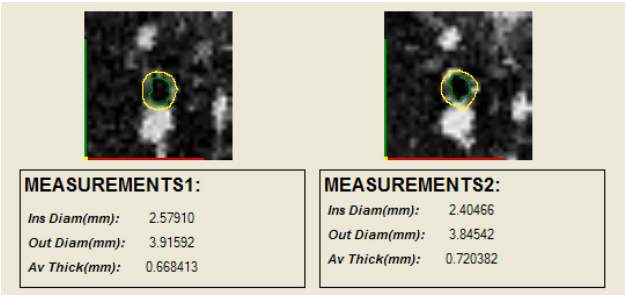

Figure 5: Measurements for the airway selected in Figure 4. Although the airway runs obliquely to the axial plane, the system determines the perpendicular plane and computes the inner (green) and outer (yellow) airway walls and diameter measurements.

For the 6 cases diagnosed with bronchiectasis, the severity of the disease was mild and even subtle. As shown in Figure 1, the automatic segmentation is able to reach more airway generations in these cases. By changing the window of the diameter coloring, the lack of tapering becomes more visible and the local evaluation correlates with the visualization (see Figures 7a and b).

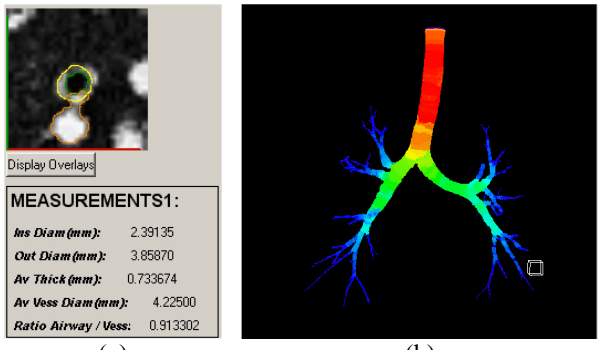

(a) (b)

Figure 6: (a) Example of airway measurement from the axial slice. (b) Bronchial tree segmentation showing a few generations of branches. The white box indicates the location of the airway analyzed in (a). Although this bronchus falls outside the automatically extracted airway tree, the system is able to perform a local evaluation of it.

Although we do not have ground truth on the locations of bronchiectasis, we were able to verify the correlation between the color changes observed in the diameter map and the corresponding broncho-arterial ratios. For an average of 92% of the locations where the color changes show an increase of the diameter, the broncho-arterial ratio is greater than one, indicating the presence of bronchiectasis (see Table 1). A 7th control patient was also evaluated, and had broncho-arterial ratios very close to one.

Patients 1 (*shown in Figure 1*) and 2 (*shown in Table 1*) have an extended airway segmentation. The

ISSN: 1727-1983

diameter map allows the easy detection of at least 20 bronchiectasis locations. For patients 3 through 6 the segmentation is not as fully developed (as shown in figure 6b) because of the presence of mucus stopping the segmentation process. Table 1 shows that although fewer spots are identified for those patients, the diameter map still accurately visualizes bronchiectasis locations. Moreover, the average bronco-arterial ratios for those patients diagnosed with mild bronchiectasis are higher than the average ratios for a healthy patient, demonstrating the usefulness of the visualization tool.

Table 1: Correlation between observed color changes in the diameter map and corresponding broncho-arterial ratio.

Patient	Reviewed locations	Average Ratio	Ratio >1	Ratio < 1
Patient 1	20	1.51+/- 0.24	90%	10%
Patient 2	27	1.52+/- 0.16	92%	8%
Patient 3	14	1.38+/- 0.22	93%	7%
Patient 4	13	1.59+/- 0.23	84%	16%
Patient 5	15	1.52+/- 0.22	93%	7%
Patient 6	8	1.35+/- 0.17	100%	0%
Healthy Patient	5	1.09+/- 0.06	80%	20%

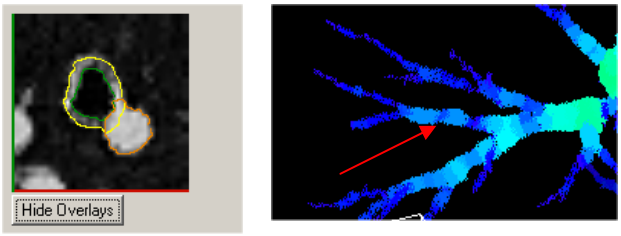

(a) (b)

Figure 7: (a) Measurements showing airway dilation. (b) Lack of tapering within the diameter visualization (red arrow).

For follow-up cases, we used 4-slice datasets, originally acquired for lung nodule monitoring or lung cancer screening. The matching function has previously been validated with 241 nodule locations in 19 pairs of datasets. 91% of predicted locations had an error less than 5mm, measured in Euclidean distance from the ground truth location [11, 12]. The application to airway matching is natural since the technique is based on surrounding surfaces and is not specific to nodules.

Although the absence of airway abnormalities in those patients prevents the demonstration of any specific airway monitoring results, the accuracy of the matching allows us to anticipate that this feature will prove highly useful in monitoring airway disease.

The bronchiectasis cases analyzed for this work were characterized by subtle dilation of the airways, which may well be missed by radiologists during routine examination. Nevertheless, our system was able to highlight areas of mild dilation within the bronchial tree. Moderate or severe cases will give rise to even more visible anomalies in the color diameter map. Although severe airway disease is unlikely to be missed by radiologists, the graphical display still provides the benefit of illustrating the extent and location of such changes.

Discussion

Thin-section CT has proved to be a principal means for the evaluation of lung disease and its use in the diagnosis of bronchiectasis and mucus plugging has clearly been demonstrated [13]. Thanks to the near-isotropic resolution of the datasets, we are able to accurately extract the bronchial tree for better airway evaluation in any plane of the 3D volume space.

In the case of bronchiectasis, the radiologist needs to assess a lack of tapering along the airways. The adjustable color diameter map of the bronchial tree allows a rapid identification of abnormalities in airway tapering. A good diameter map is dependent on the depth of the airway tree segmentation as well as the voxel resolution and sharpness of kernel reconstruction.

For those patients with bronchiectasis, the segmentation often reaches farther within the airways since the airways are dilated. Indeed, the depth of the automatic segmentation or the number of generations reached may be an indicator of the presence of abnormal dilation, how severely the patient is affected, and the locations within the bronchial tree. As a complement to global indicators such as FEV and FVC, which give a global evaluation of lung capacity and function, this visualization tool shows where within the lungs the abnormalities are located. This additional knowledge can then be brought to bear upon patient treatment.

The presence of bronchiectasis may be clinically detected and confirmed by comparing the airway diameter to the accompanying artery diameter. The local evaluation feature offered by our system accurately provides the cross-sectional diameter of the airway and the broncho-arterial ratio. We recognize that in some cases the arteries themselves may be abnormally dilated or constricted, in which case the broncho-arterial ratio is an unreliable indicator of bronchiectasis. Ultimately the clinician must confirm any visualization-based findings by examination of the original CT data, and our system

ISSN: 1727-1983

provides a simple means to do so by indicating corresponding locations.

Finally, our system is able to find the airway counterpart in two datasets of the same patient taken at different time points. This is important to monitor the treatment response or the progression of disease.

Conclusions

We have presented a system to allow rapid identification of areas of possible airway abnormalities, automatic quantification of the severity of disease, and rapid assessment of changes over time. We anticipate this will provide a valuable tool to radiologists in the assessment of disease progression and response to treatment.

Our on-going work includes further automation of measurements throughout the airway tree and clinical validation.

References

1. BHALLA M. , TURCIOS N., APONTE V., JENKINS M., LEITMAN B., MCCAULEY D. and NAIDICH D. (1991) "Cystic Fibrosis: Scoring system with Thin Section CT" Radiology 1991 179:783-788
2. KIRALY A.P., MCLENNAN G., HOFFMAN E.A., REINHARDT J.M., and HIGGINS W.E., (2002) "Three-dimensional human airway segmentation methods for clinical virtual bronchoscopy." *Academic Radiology*, 2002. 9(10): p. 1153-1168.
3. FETITA C.I., PRETEUX F., BEIGELMAN-AUBRY C., and GRENIER P., (2004) "Pulmonary airways: 3-D reconstruction from multislice CT and clinical investigation," vol. 23, no. 11, *IEEE Trans. Medical Imaging,* Nov. 2004.
4. AYKAC D, HOFFMAN EA, MCLENNAN G, and REINHARDT JM, (2003) "Segmentation and analysis of the human airway tree from three-dimensional X-ray CT images." *IEEE Trans. Medical Imaging*, 22(8):940-950, Aug. 2003.
5. TSCHIRREN J, HOFFMAN EA, MCLENNAN G, AND SONKA M, (2004) "Airway tree segmentation using adaptive regions of interest," *Medical Imaging 2004: Physiology, Function, and Structure from Medical Images*, Vol. 5369.
6. SCHLATHOLTER, T., LORENZ, C., CARLSEN, I., RENISCH, S. and DESCHAMPS, T. (2002) "Simultaneous segmentation and tree reconstruction of the airways for virtual bronchoscopy." *Image Processing. Volume 4684 of SPIE Medical Imaging*. (2002) 103–113.
7. WIEMKER R., BLAFFERT T., BULOW T., RENISCH S. and LORENZ C. (2004): "Automated assessment of bronchial lumen, wall thcikeness and bronchioarterial diameter ratio of the tracheobronchonchial tree using high-resolution CT" *Computer Assisted Radiology and Surgery* 2004, International Congress Series 1268 967-972.
8. BERGER P., PEROT V., DESBARATS P., TUNON-DE-LARA J. M., MARTHAN R. and LAURENT F. (2005) "Airway wall Thickness in Cigarette Smokers: Quantitative Thin-Section CT Assessment", *Radiology* 2005 235:1055-1064.
9. KIRALY A.P., REINHARDT J.M., HOFFMAN E.A., MCLENNAN G and HIGGINS W.E., (2005) "Virtual bronchoscopy for quantitative airway analysis", SPIE Conf. on Medical Imaging, vol. 5746, pg. 369-383, 2005.
10. KIRALY A.P., HELFERTY J.P., HOFFMAN E.A., MCLENNAN G., and HIGGINS W.E. (2004) "Three-Dimensional Path Planning for Virtual Bronchoscopy." In *IEEE Transactions on Medical Imaging*.vol. 23, no. 1, November 2004: p. 1365-1379.
11. NOVAK C.L., SHEN H., ODRY B.L., FAN L., QIAN J. and NAIDICH D.P. (2002) : "Performance of an Automatic System for Nodule Correspondence in Follow-up CT Studies of the Lung," *Annual Meeting of Radiological Society of North America* (RSNA), Chicago, IL, December 2002.
12. SHEN H., FAN L., QIAN J., ODRY B.L., NOVAK C.L. and NAIDICH D.P. (2002) : "Real-time and automatic matching of pulmonary nodules in follow-up multi-slice CT studies," *International Conference on Diagnostic Imaging and Analysis* (ICDIA), Shanghai, August, 2002.
13. GRENIER P., MAURICE F., MUSSET D., MENU Y. and NAHUM H. (1986) "Bronchiectasis: assessment by thin section CT." Radiology 1986 161:95-99

ISSN: 1727-1983